SYNTHESIS, SPECTROSCOPIC CHARACTERIZATION, SOLVENT-DEPENDENT KETO–ENOL TAUTOMERISM, AND ELECTROCHEMICAL BEHAVIOR OF OXADIAZOLE- AND TRIAZOLE-LINKED β-KETO ESTERS

Khalid K. Shaker*, Athraa H. Mekky, Wathiq S. Abdul-Hassan

Department of Chemistry, College of Science, University of Thi-Qar, Thi-Qar 64001, Iraq
e-mail: Khaled.shaker@utq.edu.iq; Wathiq.a_chem@sci.utq.edu.iq; Athraa84_chem@sci.utq.edu.iq

Received 11.10.2025
Accepted 19.05.2026

Abstract: *Four β-keto ester derivatives containing 1,2,4-triazole (A7 and A8) or 1,3,4-oxadiazole (A13 and A14) thioether units were synthesized by S-alkylation of the corresponding thiol/thione precursors with ethyl 4-chloro-3-oxobutanoate in ethanol using sodium acetate as a stoichiometric basic additive. The proposed structures are supported by FT-IR, ^{1}H NMR, and ^{13}C NMR data, including disappearance of the precursor S–H resonances and appearance of signals attributable to the β-keto ester fragment. Solvent-dependent keto–enol behavior was examined qualitatively by ^{1}H NMR spectroscopy in DMSO-d_6 and $CDCl_3$ at 298 K. Only keto-form diagnostic resonances were resolved in DMSO-d_6. In $CDCl_3$, A7 displayed signals of both keto and enol species; A8 and A14 displayed resolved enol-form signals without a resolved keto methylene signal; and A13 retained a resolved keto methylene signal without detectable enol resonances. UV/Vis spectra showed intense absorptions mainly in the ultraviolet region and weaker solvent- and concentration-sensitive features at longer wavelengths. Cyclic voltammetry in DMF containing 0.10 M tetrabutylammonium perchlorate revealed multiple cathodic processes that were predominantly irreversible on the experimental time scale. Because the Ag quasi-reference electrode was not calibrated against an internal ferrocene standard, the electrochemical results are interpreted comparatively within this data set rather than as absolute formal potentials. The combined results demonstrate qualitative relationships among heterocycle identity, methoxy substitution, solvent-dependent tautomeric signatures, and electrochemical response.*

Keywords: *β-keto esters; 1,2,4-triazoles; 1,3,4-oxadiazoles; keto–enol tautomerism; cyclic voltammetry; solvent effects*

DOI: 10.65382/2221-8688-2027-1-149-169

1. Introduction

1,3-Dicarbonyl compounds contain two carbonyl groups separated by a carbon atom and include β-diketones, β-keto esters, and related derivatives. Pentane-2,4-dione (acetylacetone) is the simplest widely studied β-diketone [1-5], whereas the target compounds of the present work belong specifically to the β-keto ester subclass. A defining feature of many 1,3-dicarbonyl systems is keto–enol tautomerism, in which proton transfer and π-bond rearrangement interconvert keto and enol forms [6,7]. The enol tautomer can be stabilized by conjugation and by a six-membered intramolecular O–H···O hydrogen bond (Figure 1). The position of the keto–enol equilibrium depends on substituent electronics and sterics, temperature, concentration, solvent, and phase [8]. Polar, strongly hydrogen-bond-accepting solvents can stabilize the more polar keto form and compete with intramolecular hydrogen bonding, whereas less polar solvents often favor internally hydrogen-bonded enol species. These tendencies are system dependent and should not be treated as universal. Because tautomerism changes electron distribution, acidity, and donor-atom geometry, it can influence chemical reactivity and metal-ion coordination. β-Dicarbonyl compounds and their conjugate bases are consequently important ligands, extraction reagents, and precursors in

coordination and materials chemistry [9-11]. Linking β-dicarbonyl groups to nitrogen- and oxygen-containing heterocycles provides a means of tuning both tautomeric and electronic properties. In particular, 1,2,4-triazole and 1,3,4-oxadiazole rings are compact, electron-deficient heteroaromatic units that can alter molecular polarity, hydrogen-bonding ability, and redox response [12–16]. Their combination with a β-keto ester fragment also introduces several potential coordination sites within a single molecule.

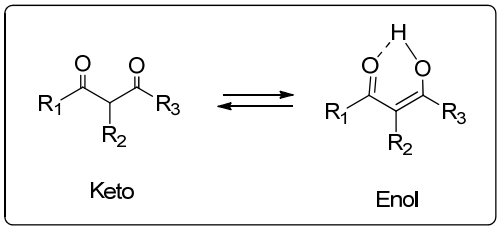

Fig. 1. General keto–enol tautomerism of a 1,3-dicarbonyl compound

Although triazole- and oxadiazole-containing compounds are widely investigated, comparatively few studies have examined molecules in which these heterocycles are connected through sulfur to a β-keto ester unit. Such systems are suitable for combined spectroscopic and electrochemical analysis because changes in solvation and tautomeric state can alter the local electronic environment and the observed reduction response [17-20]. A reliable interpretation requires complementary methods. NMR spectroscopy can distinguish resolved keto- and enol-form proton environments; FT-IR spectroscopy can support formation of the ester and ketone functionalities; UV–visible spectroscopy probes solvent- and concentration-dependent electronic absorption; and cyclic voltammetry identifies electrochemical events and their apparent reversibility under specified conditions. These methods provide qualitative structure–tautomerism–redox relationships, although definitive molecular-formula confirmation requires complementary analytical data such as high-resolution mass spectrometry and/or elemental analysis [21-24]. In this work, four β-keto ester derivatives were prepared: two 1,2,4-triazole-linked compounds (A7 and A8) and two 1,3,4-oxadiazole-linked compounds (A13 and A14). Their proposed structures were evaluated by FT-IR, ^{1}H and ^{13}C NMR spectroscopy. Solvent-dependent keto-enol signatures were compared in DMSO-d_6 and $CDCl_3$ at 298 K, while UV/Vis absorption in several solvents and cyclic voltammetric behavior in DMF were examined.

2. Experimental part

2.1. Materials and Instrumentation. Ethyl 4-methoxybenzoate, ethyl benzoate, potassium hydroxide, sodium azide, ethyl 4-chloro-3-oxobutanoate, sodium acetate, and phenyl isothiocyanate were obtained from commercial suppliers and used as received unless otherwise stated. Ethanol, ethyl acetate, n-hexane, chloroform, and methanol were supplied by Alpha Chemika, and 80% hydrazine hydrate was supplied by Scharlau. FT-IR spectra were recorded as KBr pellets on a Bruker Tensor 27 spectrometer over 4000–400 cm^{-1}. UV/Vis spectra were measured with a PG Instruments T90+ spectrophotometer using 1 cm quartz cuvettes; the solvent and nominal concentration used for each measurement is listed in Table 3. Melting points were determined with a Gallenkamp MFB-600 apparatus and are uncorrected. ^{1}H and ^{13}C NMR spectra were recorded on a Bruker Ascend 400 spectrometer at 400 and 101 MHz, respectively, using DMSO-d_6 or $CDCl_3$ as specified. Chemical shifts (δ) are reported in ppm and coupling constants (J) in hertz. Cyclic voltammetry was performed at 298 K under argon with a PARSTAT 4000 potentiostat/galvanostat using a one-compartment, three-electrode cell. A 3 mm glassy-

carbon disk, platinum wire, and silver quasi-reference electrode served as the working, counter, and reference electrodes, respectively. The supporting electrolyte was 0.10 M tetrabutylammonium perchlorate (TBAP) in DMF, and the nominal analyte concentration was 1.0 mM. Scan rates of 0.10 and 0.30 V s^{-1} were used where reported. Before each experiment, the working electrode was polished with 0.05 μm alumina slurry and rinsed with DMF. Potentials are reported versus the Ag quasi-reference electrode. We have to note that, these values are used only for comparisons within the present data set and are not treated as formal redox potentials.

2.2. Synthesis

2.2.1. Compounds A1 and A2. Compounds A1 and A2 were prepared according to a reported procedure [14, 25]. A1 (benzohydrazide): FT-IR (KBr, ν, cm^{-1}) 3300, 3225 (NH_2), 3197 (N–H), 3049 (Ar–H), 1662 (amide C=O), 1447 (N–N). A2 (4-methoxybenzohydrazide): FT-IR (KBr, ν, cm^{-1}) 3315, 3210, 3185 (NH_2/N–H), 3059, 3019 (Ar–H), 2962, 2935, 2908 (aliphatic C–H), 1651 (amide C=O). ^{1}H NMR (400 MHz, DMSO-d_6) δ 9.68 (s, 1H, CONH), 7.83 (d, J = 8.9 Hz, 2H, Ar–H), 6.97 (d, J = 9.0 Hz, 2H, Ar–H), 4.48 (s, 2H, NH_2), 3.77 (s, 3H, OCH_3). ^{13}C NMR (101 MHz, DMSO-d_6) δ 165.89 (CONH), 161.57 (Ar–C–O), 128.89, 125.26, 113.63 (aromatic C), 55.36 (OCH_3) [25–29].

2.2.2. Compounds A3 and A4. The N-acyl-N′-phenylthiosemicarbazide derivatives A3 and A4 were prepared according to the literature [21]. A3 (2-benzoyl-N-phenylhydrazine-1-carbothioamide): FT-IR (KBr, ν, cm^{-1}) 3313, 3220, 3182 (N–H), 3092, 3058 (Ar–H), 1669 (amide C=O), 1601, 1566, 1523, 1445 (aromatic-ring vibrations), 1219 (C=S), 798, 759, 707, 682 (Ar–H out-of-plane bending). ^{1}H NMR (400 MHz, DMSO-d_6) δ 11.08 (s, 1H, CONH), 10.57 (s, 1H, NH), 9.74 (s, 1H, NH), 7.98–7.16 (m, 10H, Ar–H). ^{13}C NMR (101 MHz, DMSO-d_6) δ 181.11 (C=S), 165.99 (CONH), 139.26, 132.94, 132.53, 128.46, 127.00, 126.08, 125.06, 123.00 (aromatic C). A4 [2-(4-methoxybenzoyl)-N-phenylhydrazine-1-carbothioamide]: FT-IR (KBr, ν, cm^{-1}) 3274, 3216, 3165 (N–H), 3059, 3003 (Ar–H), 2966, 2938 (aliphatic C–H), 1665 (amide C=O), 1630, 1512 (aromatic-ring vibrations), 1263 (C=S), 1221 (Ar–O–CH_3), 849, 788, 692 (Ar–H out-of-plane bending). ^{1}H NMR (400 MHz, DMSO-d_6) δ 10.44, 9.83, 9.71 (each s, 1H, NH), 7.95–7.05 (m, 9H, Ar–H), 3.82 (s, 3H, OCH_3). ^{13}C NMR (101 MHz, DMSO-d_6) δ 181.16 (C=S), 165.63 (CONH), 162.11 (Ar–C–O), 139.31, 129.91, 127.98, 126.11, 125.11, 124.73, 113.51 (aromatic C), 55.48 (OCH_3) [15, 30-32].

2.2.3. Compounds A5 and A6. A 4.0 M NaOH solution (12 mL) was added to a solution of A3 or A4 (10 mmol) in absolute ethanol (80 mL). The mixture was refluxed for 6 h, and reaction progress was monitored by TLC using ethyl acetate: n-hexane (7:3). The solution was acidified with 10% aqueous acetic acid and cooled. The precipitate was collected, washed with water, and recrystallized from water [25,33]. A5 (4,5-diphenyl-4H-1,2,4-triazole-3-thiol): FT-IR (KBr, ν, cm^{-1}) 3071, 3057 (Ar–H), 2747 (S–H), 1546, 1508, 1494, 1460 (aromatic-ring vibrations), 1499, 1446 (C=N), 1445 (N–N), 1243 (C–N), 853, 769, 701, 689 (Ar–H out-of-plane bending). ^{1}H NMR (400 MHz, DMSO-d_6) δ 14.16 (s, 1H, SH), 7.49–7.30 (m, 10H, Ar–H). ^{13}C NMR (101 MHz, DMSO-d_6) δ 168.58 (C–SH/C=S tautomeric carbon), 150.55 (C=N), 134.56, 130.36, 129.43, 129.34, 128.75, 128.57, 128.25, 125.00 (aromatic C). A6 [5-(4-methoxyphenyl)-4-phenyl-4H-1,2,4-triazole-3-thiol]: FT-IR (KBr, ν, cm^{-1}) 3015 (Ar–H), 2979, 2939 (aliphatic C–H), 2752 (S–H), 1611, 1581 (C=N), 1548, 1515 (aromatic-ring vibrations), 1463 (N–N), 1243 (Ar–O–CH_3), 837, 776, 699 (Ar–H out-of-plane bending). ^{1}H NMR (400 MHz, DMSO-d_6) δ 14.08 (s, 1H, SH), 7.49–6.88 (m, 9H, Ar–H), 3.72 (s, 3H, OCH_3). ^{13}C NMR (101 MHz, DMSO-d_6) δ 168.40 (C–SH/C=S tautomeric carbon), 160.64 (Ar–C–O), 150.50 (C=N), 134.73, 129.79, 129.15, 128.81, 117.97, 114.06 (aromatic C), 55.32 (OCH_3) [34].

2.2.4. General Procedure for A7 and A8. A mixture of A5 or A6 (10 mmol) and sodium acetate (1.36 g, 15 mmol; stoichiometric basic additive) in absolute ethanol (50 mL) was heated for 15 min. Ethyl 4-chloro-3-oxobutanoate (2.4 mL, 2.46 g, 15 mmol) was added, and the mixture was maintained at 60–70 °C for 20 h. Reaction progress was monitored by TLC using ethyl acetate: n-hexane

(7:3). The mixture was poured onto crushed ice; the precipitated product was filtered, washed with water, and recrystallized. A7 [ethyl 4-[(4,5-diphenyl-4H-1,2,4-triazol-3-yl) sulfanyl]-3-oxobutanoate]: FT-IR (KBr, ν, cm^{-1}) 3071, 3057 (Ar–H), 2997–2908 (aliphatic C–H), 1737 (ester C=O), 1719 (ketone C=O), 1625, 1592 (C=N), 1549, 1530, 1475 (aromatic-ring vibrations), 1448 (N–N), 1261 (C–O), 851, 776, 699, 631 (Ar–H out-of-plane bending). ^{1}H NMR (400 MHz, DMSO-d_6) δ 7.57–7.34 (m, 10H, Ar–H), 4.37 (s, 2H, S–CH_2), 4.11 (q, J = 7.1 Hz, 2H, OCH_2CH_3), 3.83 (s, 2H, $COCH_2CO$), 1.19 (t, J = 7.1 Hz, 3H, CH_3). ^{13}C NMR (101 MHz, DMSO-d_6) δ 197.47 (ketone C=O), 166.76 (ester C=O), 154.40, 151.23, 133.68, 130.17, 130.05, 129.78, 128.58, 127.87, 127.57, 126.49 (heteroaromatic/aromatic C), 60.70 (OCH_2), 47.77 (S–CH_2), 41.80 ($COCH_2CO$), 13.99 (CH_3). A8 [ethyl 4-{[5-(4-methoxyphenyl)-4-phenyl-4H-1,2,4-triazol-3-yl]sulfanyl}-3-oxobutanoate]: FT-IR (KBr, ν, cm^{-1}) 3061 (Ar–H), 2971–2840 (aliphatic C–H), 1740 (ester C=O), 1721 (ketone C=O), 1613, 1578 (C=N), 1536, 1482 (aromatic-ring vibrations), 1440 (N–N), 1258 (C–O), 814, 773, 711 (Ar–H out-of-plane bending). ^{1}H NMR (400 MHz, DMSO-d_6) δ 7.57–6.89 (m, 9H, Ar–H), 4.34 (s, 2H, S–CH_2), 4.10 (q, J = 7.1 Hz, 2H, OCH_2CH_3), 3.82 (s, 2H, $COCH_2CO$), 3.72 (s, 3H, OCH_3), 1.19 (t, J = 7.1 Hz, 3H, CH_3). ^{13}C NMR (101 MHz, DMSO-d_6) δ 197.61 (ketone C=O), 166.85 (ester C=O), 160.30, 150.75, 133.88, 130.20, 129.40, 127.89, 118.77, 114.10 (heteroaromatic/aromatic C), 60.77 (OCH_2), 55.27 (OCH_3), 47.82 (S–CH_2), 41.84 ($COCH_2CO$), 14.09 (CH_3) [35,36].

2.2.5. Compounds A11 and A12. Compounds A11 and A12 were prepared according to a reported procedure [37, 38]. A11 (5-phenyl-1,3,4-oxadiazole-2-thiol): FT-IR (KBr, ν, cm^{-1}) 3097, 3073 (Ar–H), 2761 (S–H), 1610 (C=N), 1572, 1504, 1488 (aromatic-ring vibrations), 1457 (N–N), 1283 (C–O–C), 1101 (C=S/C–S), 770, 699 (Ar–H out-of-plane bending). ^{1}H NMR (400 MHz, DMSO-d_6) δ 14.76 (s, 1H, SH), 7.87–7.60 (m, 5H, Ar–H). ^{13}C NMR (101 MHz, DMSO-d_6) δ 177.41 (C-2, thiol/thione tautomeric carbon), 160.46 (C=N), 132.23, 129.41, 126.03, 122.46 (aromatic C). A12 [5-(4-methoxyphenyl)-1,3,4-oxadiazole-2-thiol]: FT-IR (KBr, ν, cm^{-1}) 3215 (broad N–H/S–H tautomeric region), 3099 (Ar–H), 2983, 2914 (aliphatic C–H), 1653, 1614 (C=N), 1523, 1465 (aromatic-ring vibrations), 1443 (N–N), 1252 (Ar–O–CH_3), 1172 (C=S/C–S), 837 (Ar–H out-of-plane bending). ^{1}H NMR (400 MHz, DMSO-d_6) δ 14.60 (s, 1H, SH), 7.79 (d, J = 9.0 Hz, 2H, Ar–H), 7.09 (d, J = 9.0 Hz, 2H, Ar–H), 3.82 (s, 3H, OCH_3). ^{13}C NMR (101 MHz, DMSO-d_6) δ 177.14 (C-2, thiol/thione tautomeric carbon), 162.21, 160.54 (heteroaromatic/aromatic C), 128.22, 114.84 (aromatic C), 55.55 (OCH_3).

2.2.6. General Procedure for A13 and A14. A mixture of A11 or A12 (10 mmol) and sodium acetate (1.36 g, 15 mmol; stoichiometric basic additive) was dissolved in absolute ethanol. Ethyl 4-chloro-3-oxobutanoate (2.4 mL, 15 mmol) was then added, and the mixture was heated at 60–70 °C. Reaction progress was monitored by TLC using ethyl acetate: n-hexane (3:7). The mixture was poured onto crushed ice, and the resulting solid was filtered, washed, dried, and recrystallized from water/ethanol (1:1) [39-42]. A13 [ethyl 3-oxo-4-[(5-phenyl-1,3,4-oxadiazol-2-yl) sulfanyl]butanoate]: FT-IR (KBr, ν, cm^{-1}) 3025, 3014 (Ar–H), 2976, 2880 (aliphatic C–H), 1737 (ester C=O), 1719 (ketone C=O), 1557, 1539 (C=N), 1470 (aromatic-ring vibration), 1370 (N–N), 1228 (C–O), 1092 (C–S), 750, 641 (Ar–H out-of-plane bending). ^{1}H NMR (400 MHz, DMSO-d_6) δ 7.95–7.58 (m, 5H, Ar–H), 4.57 (s, 2H, S–CH_2), 4.10 (q, J = 7.0 Hz, 2H, OCH_2CH_3), 3.86 (s, 2H, $COCH_2CO$), 1.05 (t, J = 7.0 Hz, 3H, CH_3). ^{13}C NMR (101 MHz, DMSO-d_6) δ 196.73 (ketone C=O), 167.73 (ester C=O), 166.64 (heterocyclic C), 129.21, 127.29, 122.95 (aromatic C), 60.81 (OCH_2), 47.69 (S–CH_2), 40.12 ($COCH_2CO$), 13.96 (CH_3). A14 [ethyl 4-{[5-(4-methoxyphenyl)-1,3,4-oxadiazol-2- yl]sulfanyl}-3-oxobutanoate]: FT-IR (KBr, ν, cm^{-1}) 3046 (Ar–H), 2979, 2911, 2841 (aliphatic C–H), 1758 (ester C=O), 1720 (ketone C=O), 1655, 1611 (C=N), 1590, 1561 (aromatic-ring vibrations), 1446 (N–N), 1264 (C–O), 850 (Ar–H out-of-plane bending). ^{1}H NMR (400 MHz, DMSO-d_6) δ 7.89 (d, J = 8.9 Hz, 2H, Ar–H), 7.12 (d, J = 9.0 Hz, 2H, Ar–H), 4.54 (s, 2H, S–CH_2), 4.10 (q, J = 7.1 Hz, 2H, OCH_2CH_3), 3.84 (s, 3H,

OCH_3), 3.35 (s, 2H, $COCH_2CO$), 1.18 (t, J = 7.2 Hz, 3H, CH_3). ^{13}C NMR (101 MHz, DMSO-d_6) δ 196.86 (ketone C=O), 166.67 (ester C=O), 165.14, 162.21 (heteroaromatic/aromatic C), 128.29, 115.00, 114.00 (aromatic C), 60.81 (OCH_2), 55.57 (OCH_3), 47.60 (S–CH_2), 42.07 ($COCH_2CO$), 13.98 (CH_3).

Table 1. Selected physical properties of compounds A1–A8 and A11–A14

*Compound	Molecular formula	Color	mp (°C, uncorrected)	M (g mol^{-1})	Yield (%)
A1	$C_7H_8N_2O$	White	120	136.15	80
A2	$C_8H_{10}N_2O_2$	White	148	166.18	70
A3	$C_{14}H_{13}N_3OS$	White	180	271.34	78
A4	$C_{15}H_{15}N_3O_2S$	White	194	301.36	85
A5	$C_{14}H_{11}N_3S$	Yellowish white	290	253.32	80
A6	$C_{15}H_{13}N_3OS$	White	141	283.35	88
A7	$C_{20}H_{19}N_3O_3S$	White	146	381.45	90
A8	$C_{21}H_{21}N_3O_4S$	White	177	411.48	93
A11	$C_8H_6N_2OS$	Yellowish white	225	178.21	95
A12	$C_9H_8N_2O_2S$	White	215	208.24	80
A13	$C_{14}H_{14}N_2O_4S$	Red	189	306.34	88
A14	$C_{15}H_{16}N_2O_5S$	Yellowish white	168	336.36	88

*Compound identifiers A9 and A10 are omitted to retain the numbering used in the original laboratory records and spectral labels.

3. Results and discussion

3.1. Synthesis and Spectroscopic Characterization. The synthetic sequence is summarized in Scheme 1. Cyclization of the N-acylthiosemicarbazides A3 and A4 afforded the 1,2,4-triazole-3-thiol derivatives A5 and A6, whereas the corresponding 1,3,4-oxadiazole-2-thiol derivatives A11 and A12 were obtained by the reported route. Subsequent S-alkylation with ethyl 4-chloro-3-oxobutanoate gave the target β-keto esters A7, A8, A13, and A14 in isolated yields of 88–93% (Table 1). The molecular formulas and molar masses listed for A13 and A14 were corrected to $C_{14}H_{14}N_2O_4S$ (306.34 g mol^{-1}) and $C_{15}H_{16}N_2O_5S$ (336.36 g mol^{-1}), respectively, on the basis of the proposed structures [14, 42].

Formation of the triazole-linked products A7 and A8 is supported by loss of the precursor S–H stretching bands and appearance of two carbonyl absorptions attributable to ester and ketone groups. For A7, these bands occur at 1737 and 1719 cm^{-1}; for A8, they occur at 1740 and 1721 cm^{-1}. The ^1H NMR spectra show S–CH_2 singlets at δ 4.37 (A7) and 4.34 ppm (A8), ethoxy CH_2 quartets at δ 4.11 and 4.10 ppm, β-keto ester methylene singlets at δ 3.83 and 3.82 ppm, and ethyl CH_3 triplets at δ 1.19 ppm. The corresponding ^{13}C NMR spectra contain ketone carbonyl signals at δ 197.47 and 197.61 ppm and ester carbonyl signals at δ 166.76 and 166.85 ppm. Signals assigned to S–CH_2, $COCH_2CO$, OCH_2, and CH_3 occur in the expected aliphatic regions. Taken together, these data are consistent with S-alkylation of A5 and A6 and incorporation of the β-keto ester fragment (Fig.s 2–6) [43].

The oxadiazole-linked derivatives A13 and A14 show analogous spectroscopic changes. Their precursor S–H bands are absent, while ester/ketone carbonyl absorptions occur at 1737/1719 cm^{-1} for A13 and 1758/1720 cm^{-1} for A14. In the ^1H NMR spectra, the S–CH_2 groups resonate at δ 4.57 (A13)

and 4.54 ppm (A14), the ethoxy CH_2 groups at approximately δ 4.10 ppm, and the β-keto ester methylene groups at δ 3.86 and 3.35 ppm, respectively. The ^{13}C NMR spectra exhibit ketone/ester carbonyl pairs at δ 196.73/167.73 ppm for A13 and 196.86/166.67 ppm for A14. These observations are consistent with formation of the proposed thioether-linked β-keto esters rather than retention of the thiol/thione precursors. Definitive confirmation of elemental composition should be obtained by HRMS and/or CHNS analysis [44-46].

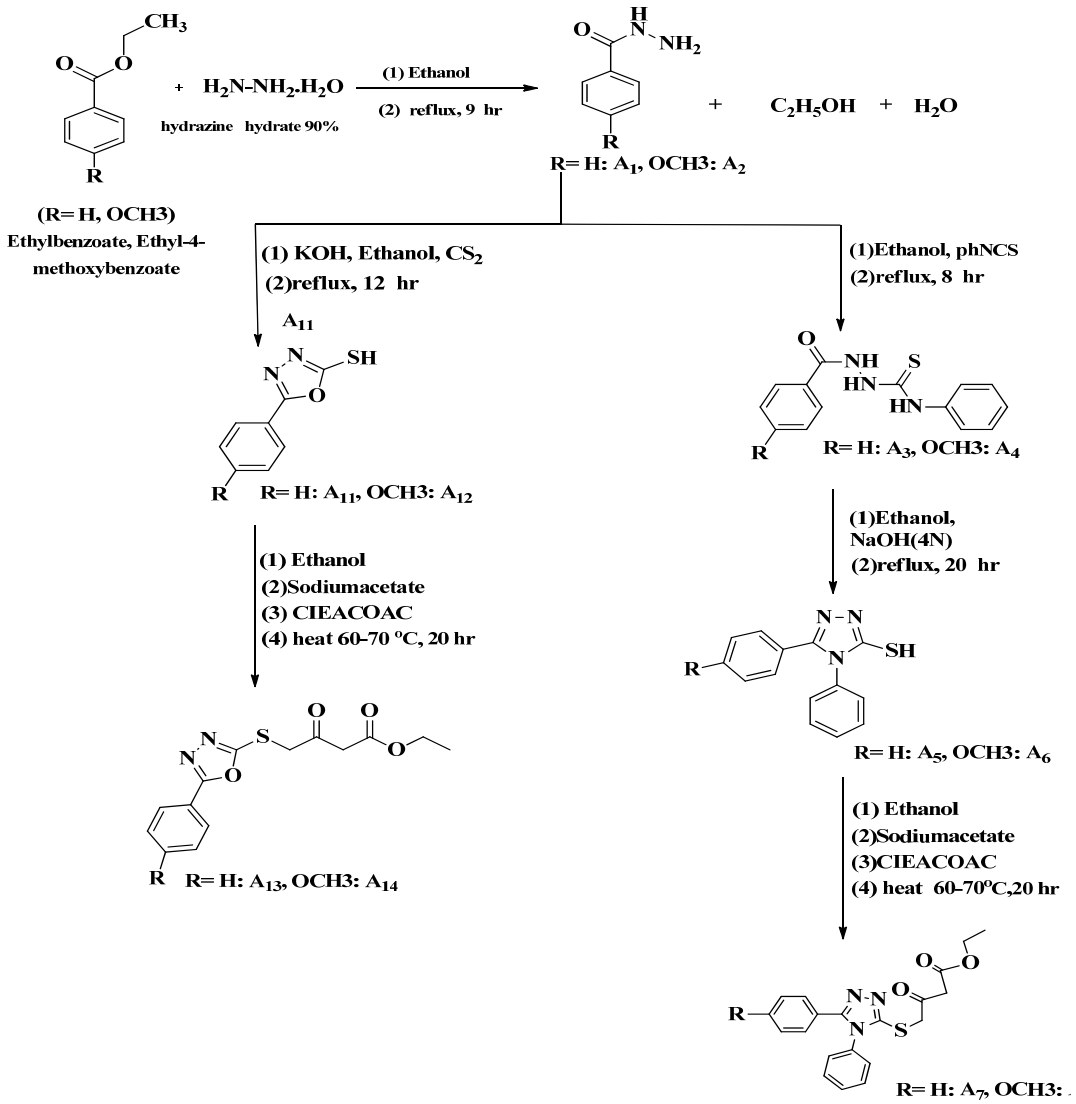

Scheme 1. Synthetic routes to compounds A1–A8 and A11–A14

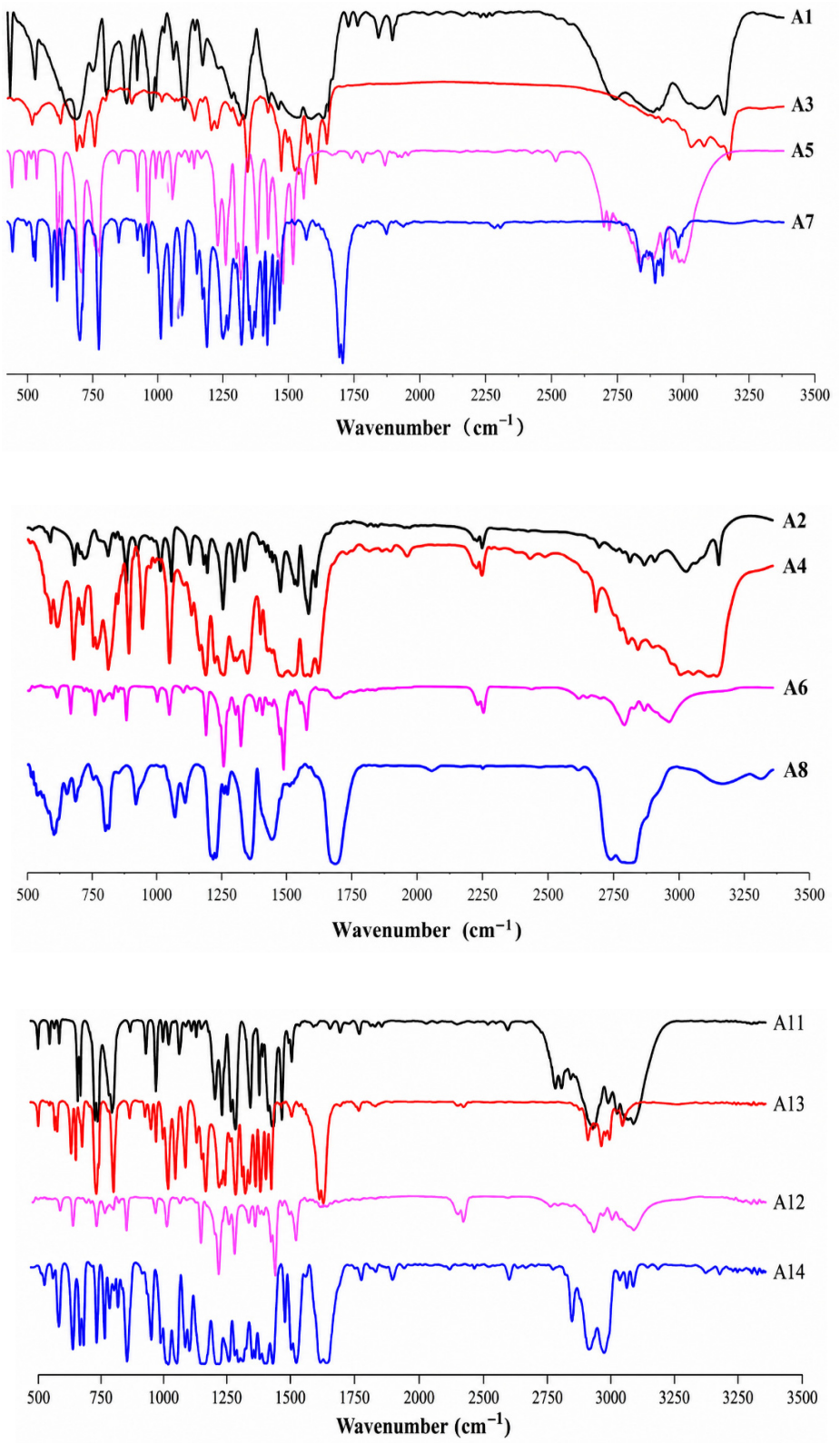

Fig. 2. FT-IR spectra of compounds A1–A8 and A11–A14

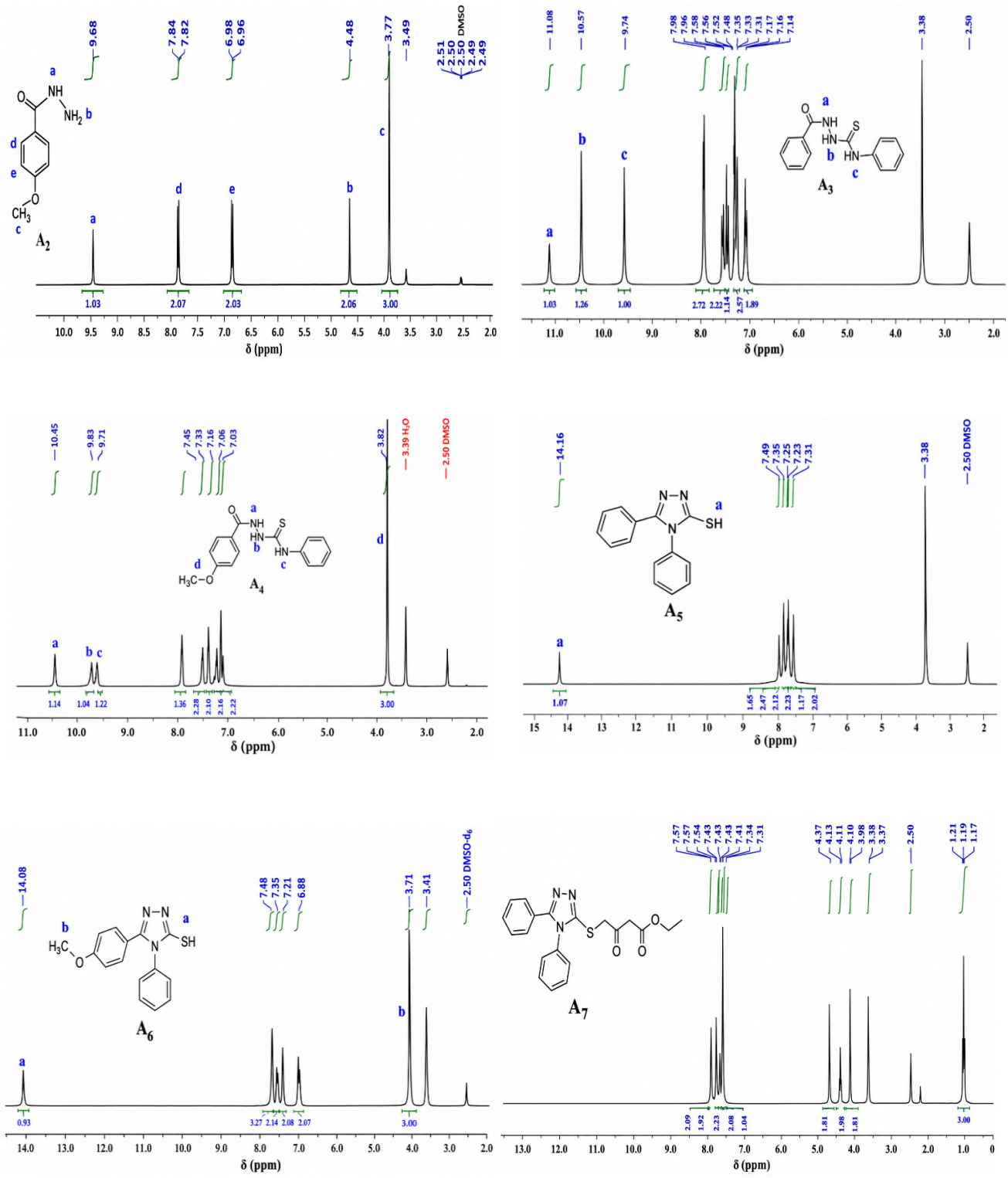

Fig. 3. ^{1}H NMR spectra (400 MHz, DMSO-d$_6$, 298 K) of compounds A2–A7

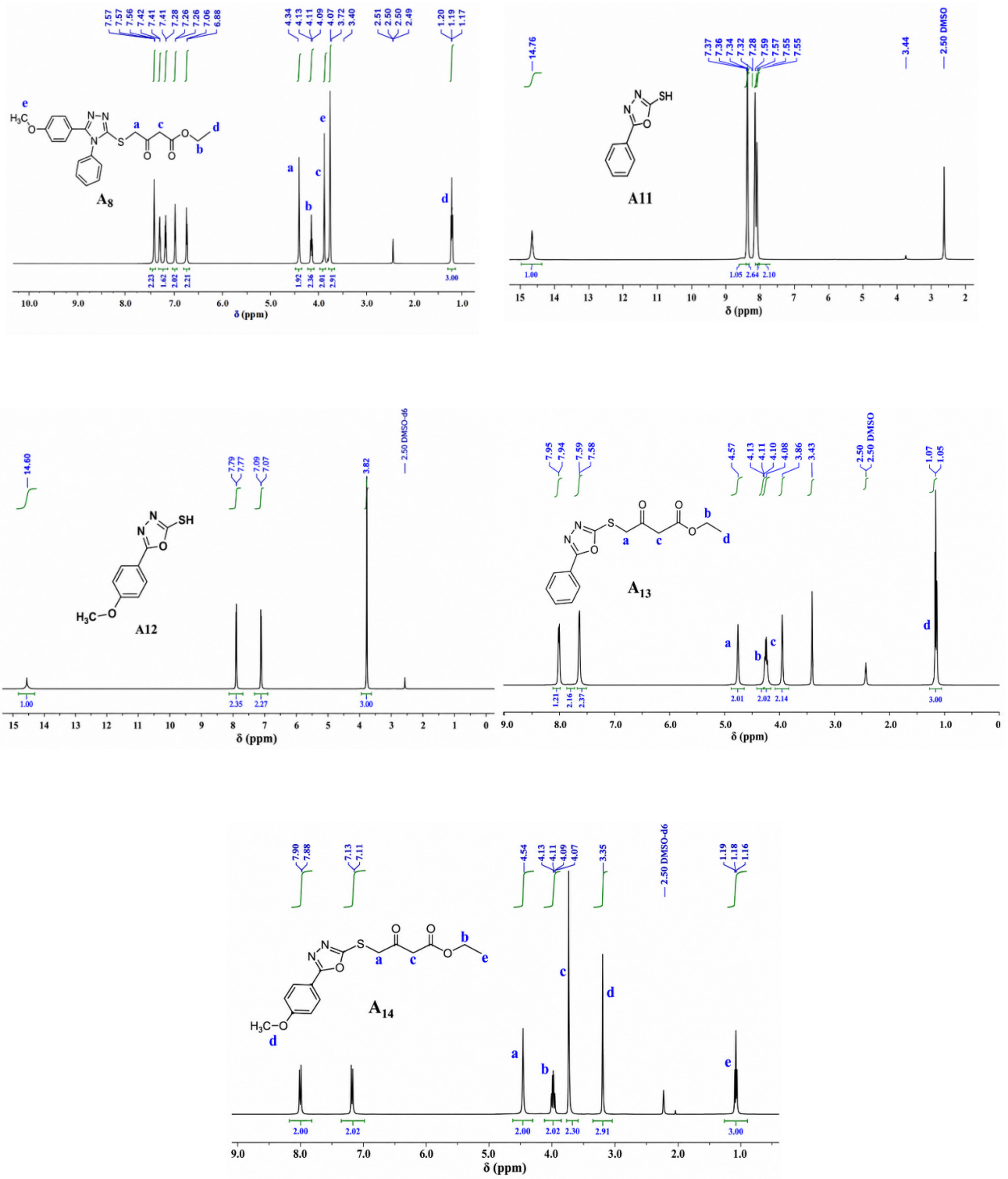

Fig. 4. ^{1}H NMR spectra (400 MHz, DMSO-d$_6$, 298 K) of compounds A8 and A11–A14

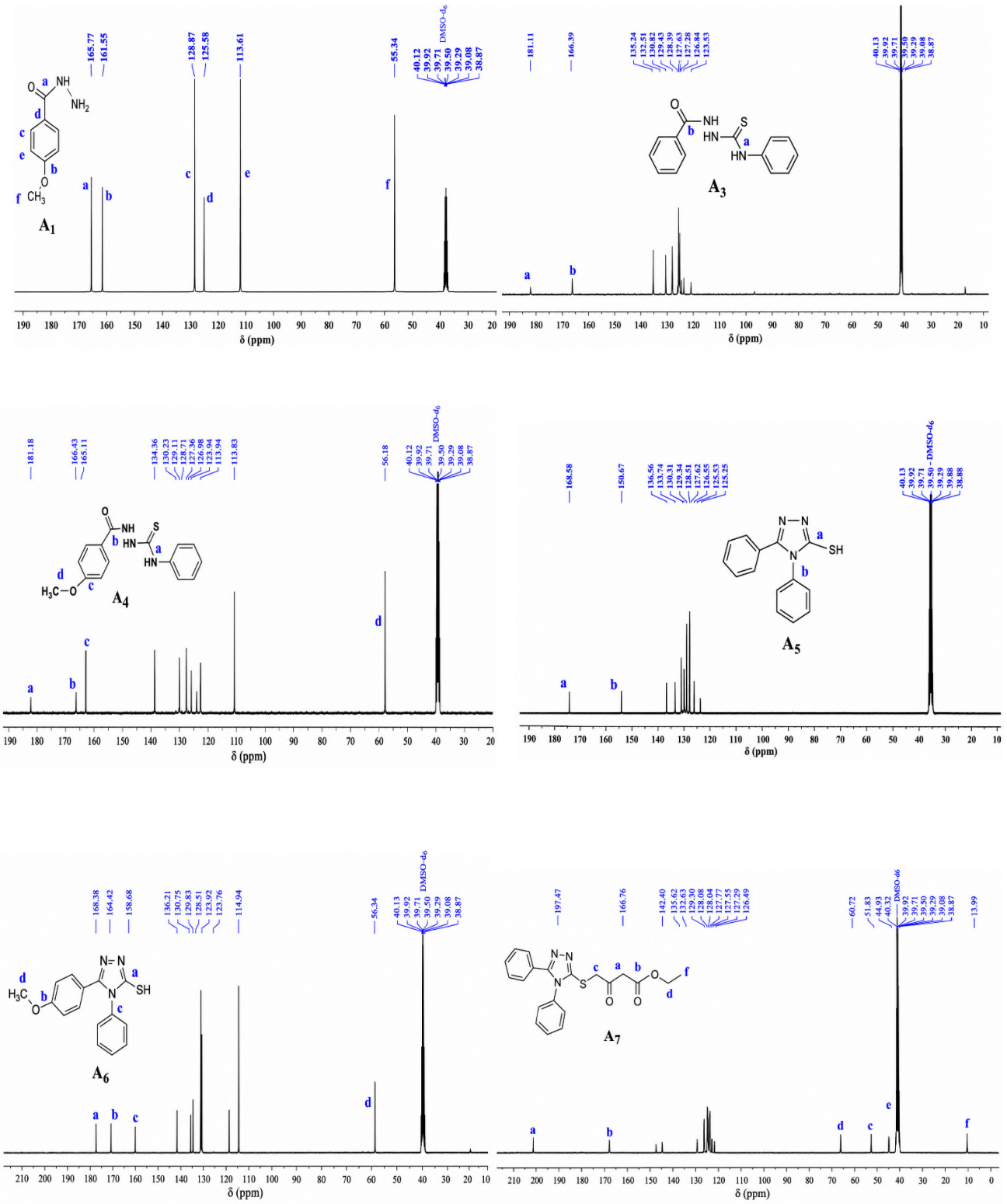

Fig. 5. ^{13}C NMR spectra (101 MHz, DMSO-d$_6$, 298 K) of compounds A2–A7

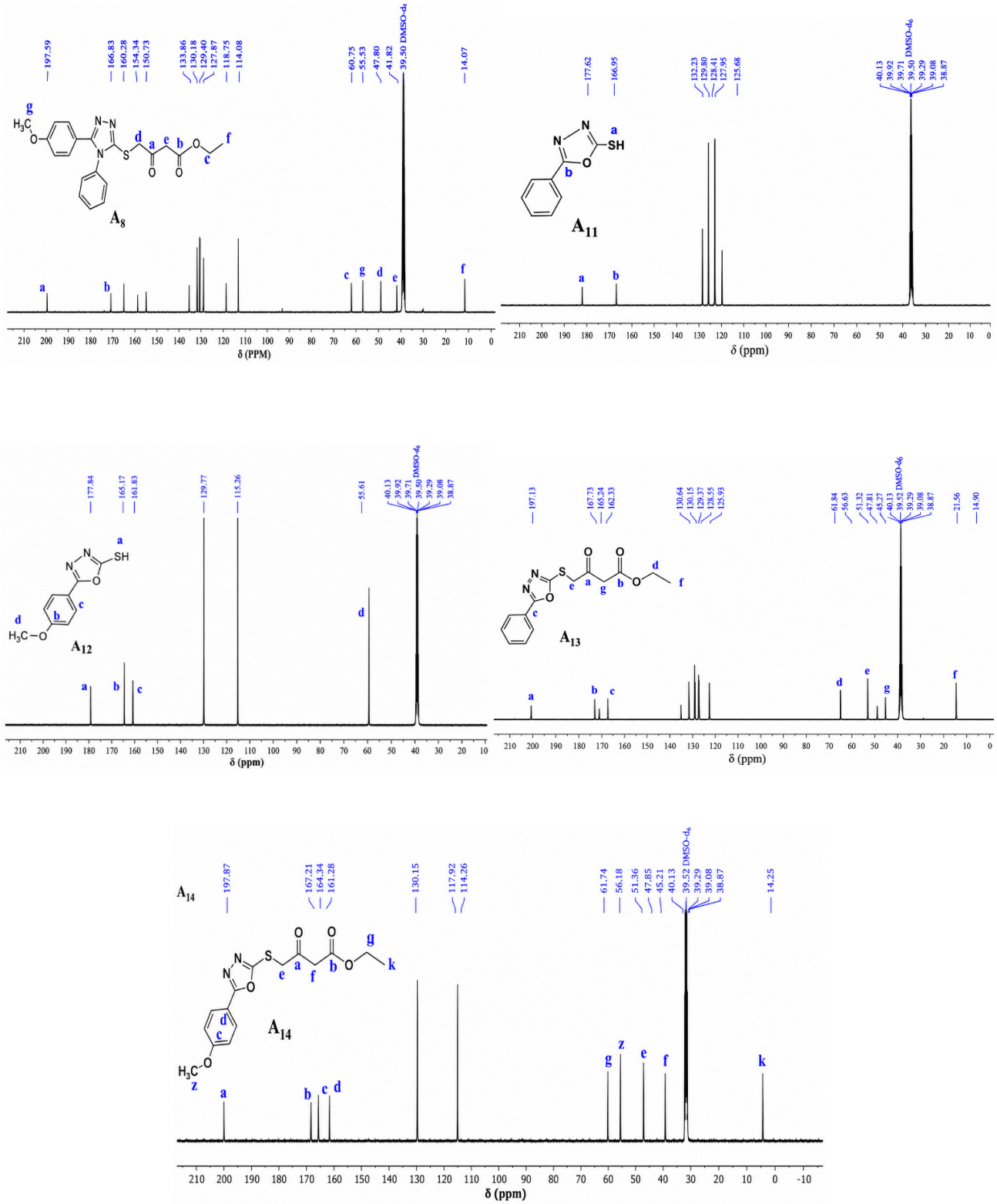

Fig. 6. ^{13}C NMR spectra (101 MHz, DMSO-d$_6$, 298 K) of compounds A8 and A11–A14

3.2. Keto–Enol Tautomerism. Keto–enol tautomerism is a prototropic equilibrium involving proton transfer and redistribution of a π bond. In DMSO-d$_6$ at 298 K, A7, A8, A13, and A14 display

resonances assigned to the methylene group of the keto β-keto ester unit, while neither a resolved strongly deshielded enolic OH signal nor a vinylic CH signal is observed. Thus, only keto-form diagnostic resonances were detected under the acquisition conditions. This is a qualitative observation; tautomer populations were not calculated because the relevant independently resolved signals were not integrated quantitatively under validated relaxation conditions [9].

Spectra acquired in $CDCl_3$ reveal detectable enol-form resonances for several compounds (Fig. 7 and Table 2). For A7, an enolic OH resonance at δ 12.04 ppm and a vinylic CH resonance at δ 5.30 ppm are observed together with a keto-form methylene signal at δ 3.20 ppm, demonstrating coexistence of spectroscopically detectable keto and enol species. The change relative to DMSO-d_6 is consistent with stabilization of an intramolecularly hydrogen-bonded enol in the less polar solvent. The remaining S–CH_2 and ethoxy resonances show only modest solvent-dependent shifts.

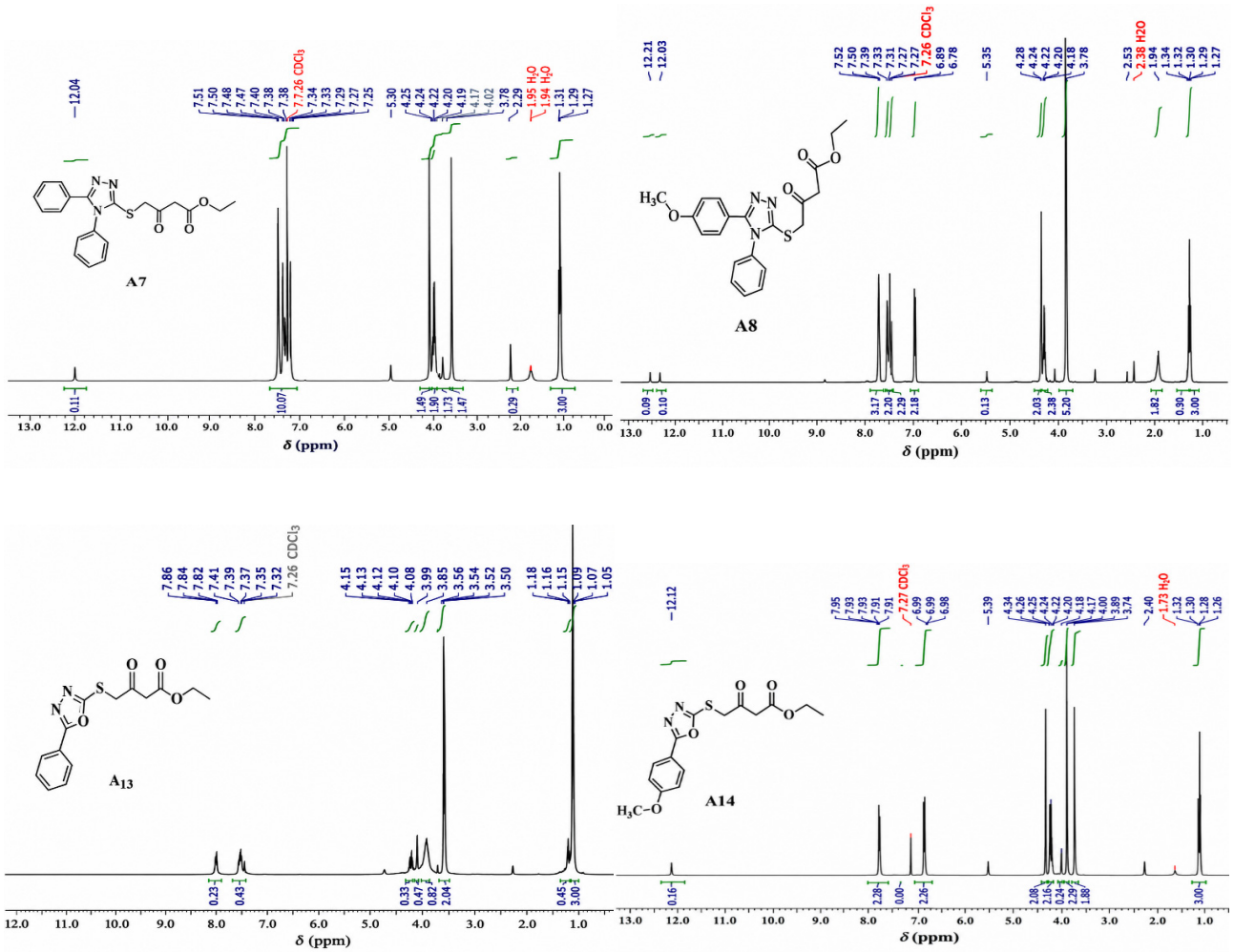

Fig. 7. ^{1}H NMR spectra (400 MHz, $CDCl_3$, 298 K) of compounds A7, A8, A13, and A14

For A14 in $CDCl_3$, signals at δ 12.12 ppm (hydrogen-bonded OH) and 5.30 ppm (vinylic CH) are observed, whereas a separate keto methylene resonance is not resolved. This pattern is consistent with an enol-dominated spectrum, but a numerical tautomer ratio cannot be assigned from the available data. In contrast, A13 retains a resolved keto methylene signal in both DMSO-d_6 and $CDCl_3$ and shows no resolved enolic OH or vinylic CH signal under the conditions used; therefore, no enol contribution was detected spectroscopically for A13. For A8 in $CDCl_3$, the keto methylene

resonance is not resolved, whereas a vinylic signal at δ 5.30 ppm and two downfield OH resonances at δ 12.03 and 12.21 ppm are observed. These OH signals may reflect more than one hydrogen-bonded enolic environment, conformational heterogeneity, slow exchange, or a minor impurity; a unique assignment is not justified by one-dimensional ^{1}H NMR alone. D_2O-exchange, variable-temperature NMR, and COSY/HSQC/HMBC measurements are required for definitive assignment. Overall, the available spectra demonstrate qualitative solvent- and structure-dependent changes in the resolved tautomeric signatures [11].

Table 2. Selected ^{1}H NMR chemical shifts (δ, ppm) diagnostic of keto and enol forms in DMSO-d_6 and $CDCl_3$

Solvent / compound		CH_3CH_2	OCH_3	S–CH_2	O–CH_2	$COCH_2CO$	Enol CH	Enol OH
DMSO-d_6	A7	1.19	—	4.37	4.11	3.83	—	—
$CDCl_3$		1.29	—	4.22	4.12	3.20	5.30	12.04
DMSO-d_6	A8	1.19	3.72	4.34	4.10	3.82	—	—
$CDCl_3$		1.30	3.78	4.28	4.22	—	5.30	12.03, 12.21
DMSO-d_6	A13	1.05	—	4.57	4.10	3.86	—	—
$CDCl_3$		1.06	—	3.99	4.12	3.85	—	—
DMSO-d_6	A14	1.18	3.84	4.54	4.10	3.35	—	—
$CDCl_3$		1.30	3.88	4.34	4.24	—	5.30	12.12

Note: The assignments in Table 2 are based on resolved diagnostic resonances. The measurements were not acquired as validated quantitative NMR experiments; therefore, no keto/enol percentages are reported.

3.3. UV/Vis Absorption Spectroscopy. The UV/Vis absorption spectra of A7, A8, A13, and A14 were recorded in solvents of different polarity, including n-hexane, benzene, dichloromethane (DCM), 1,2-dichloroethane (1,2-DCE), chloroform, ethanol, methanol, DMF, and DMSO. The nominal concentrations used for individual spectra and the corresponding absorption maxima and reported apparent molar absorptivities are summarized in Fig. 8 and Table 3.

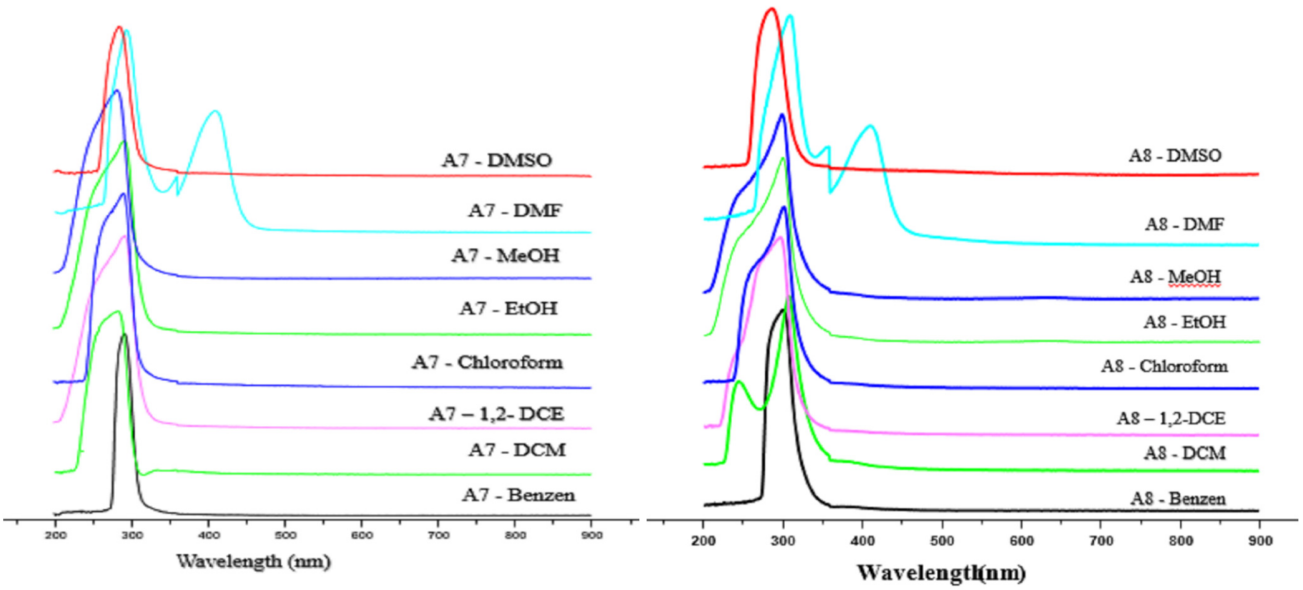

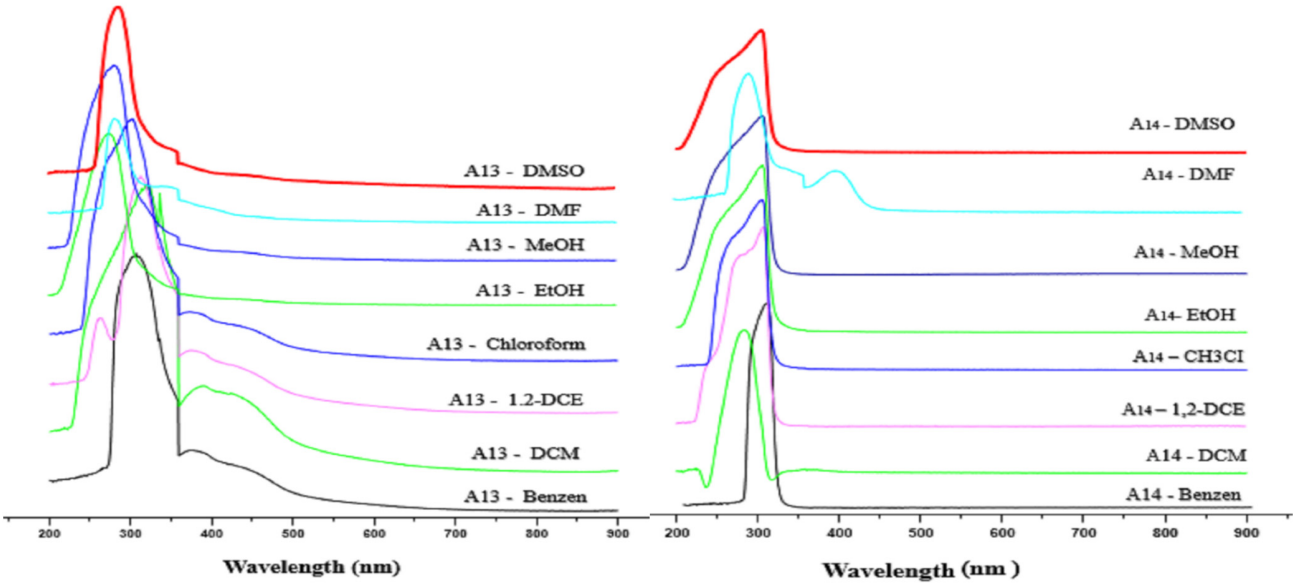

Fig. 8. UV–visible absorption spectra of A7, A8, A13, and A14 in the indicated solvents at 298 K (1 cm quartz cell)

Table 3. UV/Vis absorption maxima and reported apparent molar absorptivities of A7, A8, A13, and A14

Compound	Concentration (mM)	Solvent	λmax (nm), ε_{app} (M^{-1} cm^{-1})
A7	1.0	Benzene	290 (1400)
	1.0	DCM	284 (1300), 358 (150)
	0.10	Chloroform	290 (15 500)
	0.10	EtOH	291 (15 000)
	0.10	MeOH	281 (15 000)
	0.10	DMF	293 (17 000), 355 (4500), 409 (11 000)
	0.02		277 (2500), 405 (1000)
	0.10	DMSO	298 (12 000)
A8	0.10	Benzene	277 (15 000)
	0.40		301 (4450)
	1.0	n-Hexane	268 (1450), 380 (200)
	1.0	DCM	246 (800), 308 (1580)
	0.20	1,2-DCE	245 (4000), 289 (9000)
	0.10		288 (16 000)
	0.40	Chloroform	208 (3950), 303 (3000)
	0.40	EtOH	230 (950), 293 (3800)
	0.40	MeOH	252 (2250), 300 (4000)
	0.10	DMF	310 (2010), 359 (900), 411 (1000)
	0.20		294 (8000), 370 (1350)
	0.10	DMSO	286 (1450)
	0.05		279 (2360)
A13	1.0	Benzene	284 (1200)
	7.0		307 (314), 360 (143), 375 (142), 451 (57)

	1.0	DCM	292 (1500), 430 (100)
	7.0		329 (342), 336 (342), 390 (107), 423 (85)
	1.0	1,2-DCE	264 (500), 292 (690), 452 (50)
	7.0		260 (114), 336 (286), 362 (143), 374 (86)
	1.0	Chloroform	273 (1180)
	7.0		303 (300), 373 (57), 440 (14)
	1.0	EtOH	272 (1440), 441 (100)
	1.0	MeOH	280 (1600), 430 (100)
	1.0	DMF	281 (900), 351 (1000)
	1.0	DMSO	258 (380), 285 (1500), 446 (100)
A14	0.10	Benzene	303 (16 000)
	1.0	DCM	298 (1600), 358 (100)
	0.10		283 (8000), 359 (1000)
	0.40		296 (3750)
	0.10	1,2-DCE	236 (5500), 255 (13 000), 306 (15 000)
	0.10	Chloroform	266 (13 800), 306 (18 000)
	0.05		294 (3120)
	0.20	EtOH	253 (14 000), 306 (17 600)
	0.10		228 (2500), 293 (15 000)
	0.10	MeOH	306 (8850)
	0.20		228 (2600), 294 (15 800)
	0.10	DMF	292 (9000), 399 (2700)
	0.10	DMSO	308 (16 500)
	0.02		292 (6250)

Note: Concentrations were not uniform across all spectra. The tabulated absorptivities are therefore reported as apparent values and should not be compared quantitatively until concentration accuracy and Beer–Lambert linearity have been verified.

The dominant absorptions of the triazole-linked derivatives occur mainly between 208 and 310 nm, while those of the oxadiazole-linked derivatives occur mainly between 228 and 336 nm. Weaker features extend into the 350–452 nm region for several solvent/concentration combinations. The intense short-wavelength bands are consistent with allowed $\pi\rightarrow\pi^*$ transitions involving the heteroaromatic and aryl chromophores, whereas the weaker long-wavelength features may include contributions from $n\rightarrow\pi^*$ transitions and from different tautomeric, solvated, or associated states. These assignments are tentative in the absence of TD-DFT calculations. The spectral shifts are not monotonic with solvent polarity, and some maxima differ with concentration in the same solvent. Such behavior may reflect simultaneous effects of solvation, hydrogen bonding, tautomer distribution, association, and experimental concentration uncertainty. Therefore, the data support solvent- and concentration-sensitive electronic absorption but do not establish a single linear solvatochromic trend. Quantitative comparison of molar absorptivities requires verification of concentration accuracy and Beer–Lambert linearity at multiple concentrations [1, 47-48].

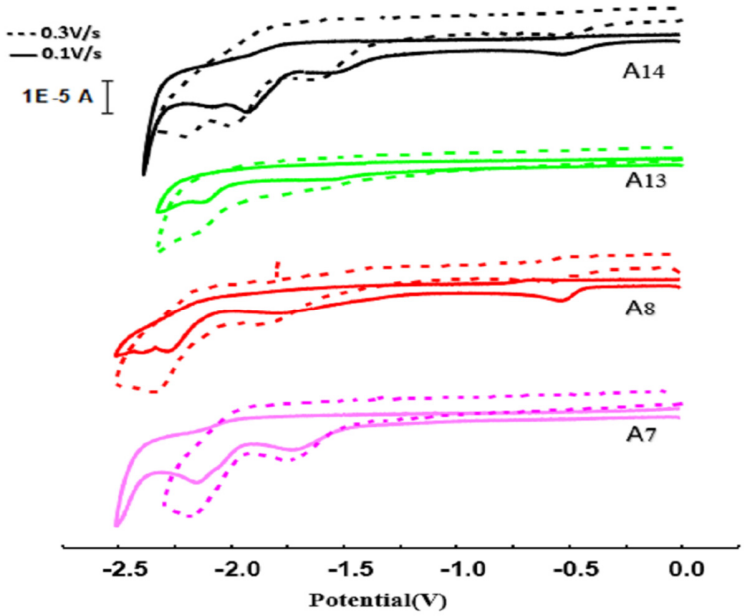

Fig. 9. Cyclic voltammograms of nominally 1.0 mM A7, A8, A13, and A14 in DMF containing 0.10 M TBAP. Scan rates of 0.10 and 0.30 V s^{-1} are shown where available. Working electrode: 3 mm glassy carbon; counter electrode: Pt wire; reference electrode: Ag quasi-reference electrode

3.4. Electrochemical Behavior. Cyclic voltammograms of A7, A8, A13, and A14 were recorded in DMF containing 0.10 M TBAP at scan rates of 0.10 and 0.30 V s^{-1} where available (Fig. 9). The solutions were deaerated with argon to minimize oxygen-related background currents. Peak potentials are reported versus the Ag quasi-reference electrode. Because an internal ferrocene standard was not reported, the absolute potential scale may drift between experiments and should not be compared directly with literature values obtained using calibrated reference systems. The peak data are therefore interpreted qualitatively within this series and are summarized in Table 4.

Table 4. Reported cyclic-voltammetric peak data for A7, A8, A13, and A14 in DMF/0.10 M TBAP

Compound	ν (V s^{-1})	Peak	E_p,fwd (V)	I_p,fwd (μA)	E_p,return (V)	I_p,return (μA)
A7	0.10	C1	−1.735	−18.359	—	—
A7	0.10	C2	−2.157	−25.310	—	—
A7	0.30	C1	−1.738	−26.545	—	—
A7	0.30	C2	−2.186	−58.220	—	—
A8	0.10	C1	−0.541	−11.264	−0.650	3.769
A8	0.10	C2	−1.780	−21.823	—	—
A8	0.10	C3	−2.280	−47.220	—	—
A8	0.10	C4	−2.390	−52.617	—	—
A8	0.30	C1	−0.551	−16.542	−0.654	4.408
A8	0.30	C2	−1.855	−8.817	—	—
A8	0.30	C3	−2.365	−6.793	—	—
A13	0.10	C1	−1.570	−4.673	—	—
A13	0.30	C1	−1.600	−25.425	—	—
A13	0.30	C2	−2.136	−12.817	—	—
A14	0.10	C1	−0.561	−6.925	—	—

Compound	ν (V s^{-1})	Peak	E_p,fwd (V)	I_p,fwd (μA)	E_p,return (V)	I_p,return (μA)
A14	0.10	C2	−1.646	−12.332	—	—
A14	0.10	C3	−2.027	−54.160	—	—
A14	0.10	C4	−2.177	−51.220	—	—
A14	0.10	C5	−2.192	−55.110	—	—

Note: Potentials are referenced to the Ag quasi-reference electrode and were not calibrated against Fc/Fc^+. Forward and return peak positions are reported without calculating $E_{1/2}$ or a formal potential for irreversible or chemically coupled processes.

All four compounds exhibit multiple cathodic waves within the accessible potential window, and most processes do not show a resolved return peak under the reported conditions. The deeper cathodic features of the methoxy-substituted derivatives generally occur at more negative potentials than those of their unsubstituted analogues, consistent with an electron-donating substituent decreasing the ease of reduction within the molecular framework. A8 and A14 also display a cathodic feature near −0.55 V that is not resolved for A7 or A13. For A8, a return peak is reported for this first event; however, the separation of the forward and return peak potentials and the small return-to-forward current ratio indicate that the event is not electrochemically reversible under these conditions. Because the potentials were not Fc/Fc^+-referenced and only two scan rates were used, no formal potentials, electron-transfer rate constants, diffusion coefficients, or mechanistic assignments are derived. Assignment of individual waves to the heterocycle, carbonyl group, or substituent would require ferrocene-referenced measurements, a wider scan-rate series, blank-electrolyte controls, controlled-potential electrolysis, and/or spectroelectrochemical characterization. The present data therefore support only qualitative substituent-dependent differences in electrochemical response and do not provide a basis for ranking nucleophilic or electrophilic reactivity [49-54].

Conclusions

Four thioether-linked β-keto ester derivatives containing 1,2,4-triazole or 1,3,4-oxadiazole units were synthesized. FT-IR and one-dimensional NMR data are consistent with S-alkylation of the heterocyclic thiol/thione precursors and formation of the proposed β-keto ester fragments. Molecular-formula confirmation by HRMS and/or elemental analysis remains necessary. The ^{1}H NMR spectra show solvent-dependent tautomeric signatures: only keto-form diagnostic resonances were resolved in DMSO-d_6; A7 showed both keto- and enol-form signals in $CDCl_3$; A8 and A14 showed resolved enol-form signals without a resolved keto methylene signal in $CDCl_3$; and A13 showed no detectable enol-form resonances under either condition. These observations are qualitative because tautomer populations were not determined.

The UV–visible spectra depend on solvent and concentration but do not follow a simple monotonic polarity trend. Cyclic voltammetry reveals several predominantly irreversible cathodic processes, and methoxy substitution is associated with changes in the number and position of the observed peaks. Because the electrochemical potentials were measured against an uncalibrated Ag quasi-reference electrode, the interpretation is restricted to internal qualitative comparisons. The present study identifies structure-dependent spectroscopic and electrochemical trends, while definitive tautomer populations, electronic-transition assignments, and reduction mechanisms require variable-temperature and multidimensional NMR, Fc/Fc^+-referenced electrochemistry, spectroelectrochemistry, HRMS/CHNS analysis, and quantum-chemical calculations.

Acknowledgments

The authors thank the Department of Chemistry, College of Science, University of Thi-Qar, for access to laboratory facilities and materials.

Conflict of interest

The authors declare no competing financial interest.

References

1. Gatea A.H., Abdul-Hassan W.S., Ali S.A., Mahdi Z.M. Ligand Adducts of Bis(acetylacetonato) Copper(II), Bis(3-chloroacetylacetonato) Copper(II) with 4,4'-bipyridine and Propylene Spacered Bis-viologen. *J. Med. Chem. Sci.* 2023, **Vol. 6(2)**, p. 280-303. DOI: 10.26655/JMCHEMSCI.2023.2.10.
2. Staniszewski B., Urbaniak W. A simple and efficient synthesis of 3-substituted derivatives of pentane-2, 4-dione. *Chem. Pap.* 2009, **Vol. 63(2)**, p. 212-216. DOI: 10.2478/s11696-008-0097-9.
3. Jassem I.A., Abdul-Hassan W.S., Flafel I.A., Ali S.A., Mahdi Z.M. Cloud point and solvent extraction of copper (II) by bis(3-chloroacetylacetone) Ethylenediimine. *J. Med. Chem. Sci.* 2022, **Vol. 5(6)**, p. 988-1000. DOI: 10.26655/JMCHEMSCI.2022.6.12.
4. Musa A.M., Abdul-Hassan W.S. Iron (II), Cobalt (II) and Nickel (II) complexes of bis- (3-chloroacetylacetonate) ethylenediimine and bis-(acetylacetonate) ethylenediimine and their viologen molecular switches. *J. Med. Pharm. Chem. Res.* 2023, **Vol. 5(6)**, p. 492-521. DOI: 10.22034/ecc.2023.370745.1556.
5. Jassem I.A., Abdul-Hassan W.S., Flafel I.A., Jghebil H.O. Axial ligation for copper (II) complexes of bis (acetylacetonato) ethylenediimine and bis (3-chloroacetylacetonato) ethylenediimine. extraction of copper by 3-chloro-2,4-pentanedione as complexing reagent. *J. Med. Pharm. Chem. Res.* 2023, **Vol. 5(2)**, p. 173-203. DOI: 10.22034/ecc.2023.363684.1533.
6. Hussain H.A., Abdul-Hassan W.S. Viologen molecular switches incorporating bis (acetylacetonato) cobalt (II) and bis (3-chloroacetylacetonato) cobalt (II) complexes. *J. Med. Pharm. Chem. Res.* 2022, **Vol. 5(7)**, p. 616-641. DOI: 10.22034/ecc.2022.370750.1557.
7. Manbeck K.A., Boaz N.C., Bair N.C., Sanders A.M.S., Marsh A.L. Substituent Effects on Keto À Enol Equilibria Using NMR Spectroscopy. *J. Chem. Educ.* 2011, **Vol. 88**, p. 1444-1445. DOI: 10.1021/ed1010932.
8. Lehrich S.W., Mahrholdt J., Korb M., Hildebrandt A., Swarts J.C., Lang H. Synthesis, characterization, and electrochemistry of diferrocenyl β-diketones, -diketonates, and pyrazoles. *Molecules,* 2020, **Vol. 25(19)**, p. 11-14. DOI: 10.3390/molecules25194476.
9. Smith K.T., Young S.C., Deblasio J.W., Hamann C.S. Measuring Structural and Electronic Effects on Keto-Enol Equilibrium in 1,3-Dicarbonyl Compounds. *J. Chem. Educ.* 2016, **Vol. 93(4)**, p. 790-794. DOI: 10.1021/acs.jchemed.5b00170.
10. Sodhi R.K., Paul S. An overview of metal acetylacetonates: developing areas/routes to new materials and applications in organic syntheses. *Catal. Surv. from Asia.* 2018, **Vol. 22**, p. 31-62. DOI: 10.1007/s10563-017-9239-9.
11. Sandler I., Harper J.B. Explanation of Substituent Effects on the Enolization of β - Diketones and β - Ketoesters. *J. Chem. Educ.* 2021, **Vol. 98(3)**, p. 1043-1048. DOI: 10.1021/acs.jchemed.0c01076.
12. Abdelrehim E.S.M. Synthesis and Screening of New [1,3,4]Oxadiazole, [1,2,4]Triazole, and [1,2,4]Triazolo[4,3- b][1,2,4]triazole Derivatives as Potential Antitumor Agents on the Colon Carcinoma Cell Line (HCT-116). *ACS Omega.* 2021, **Vol. 6(2)**, p. 1687-1696. DOI:10.1021/acsomega.0c05718

13. James L.C., Thompson D.F. An Electrosynthesis of 1,3,4-Oxadiazoles from N-Acyl Hydrazones. *Chem. Eur. J.* 2024, **Vol. 30(69)**, e202403128. DOI: 10.1002/chem.202403128.
14. Iraqi M.A., Al-Allaf H.A.I. Synthesis of Some 2-Substituted Quinazolin-4 (3H)-one Compounds from Methyl α-[(4-oxoquinazolin-2-yl)thio]acetate. *Egypt. J. Chem.* 2021, **Vol. 64(12)**, p. 7263-7270. DOI: 10.21608/EJCHEM.2021.78538.3844.
15. Hassan B.A., Mekky A.H. Synthesis, Characterization and Antibacterial Activity of [1,2,4]Triazolo[4,3-B][1,2,4,5]Tetrazine Derivatives. *Chemical Problems,* 2025, **Vol. 23(1)**, p. 78-94. DOI: 10.32737/2221-8688-2025-1-78-94.
16. Al-Juburi R.M. Synthesis and Characterization of Some Heterocyclic Compounds (Oxazepine, Tetrazole) Derived from Schiff Bases. *J. Al-Nahrain Univ. Sci.* 2012, **Vol. 15(4)**, p. 60-67. DOI: 10.22401/jnus.15.4.07.
17. Thejeel E., Mekky A.H. Synthesis, Absorption, Distribution, Metabolism, Excretion, Toxicology (Admet) and Molecular Docking Studies Of Some Pyridin-2 (1h)-One Derived From A Apocynin In Thi-Qar Governorate. *UTJsci.* 2023, **Vol. 10(2)**, p. 73-80. DOI:10.32792/utq/utjsci/v10i2.1089.
18. Kharb R., Sharma P.C., Yar M.S. Pharmacological significance of triazole scaffold. *J. Enzyme Inhib. Med. Chem.* 2011, **Vol. 26(1)**, p. 1-21. DOI: 10.3109/14756360903524304.
19. Namratha B., Gaonkar S.L. 1,2,4-Triazoles: Synthetic Strategies and Pharamacological Profiles. *Int. J. Pharm. Pharm. Sci.* 2014, **Vol. 6(8)**, p. 73-80.
20. Jampilek J. Heterocycles in Medicinal Chemistry. *Molecules,* 2019, **Vol. 24**, 3839. DOI:10.3390/molecules24213839
21. Maha D.A., Sajid H.G., Athraa H.M. Synthesis Characterization and Spectrophotometric Studies of New Hydrazone Derived from Ethyl Benzoate. *J. Glob. Pharma Technol.* 2019, **Vol. 11(07)**, p. 251-257.
22. Jasim A.M. Synthesis, Characterization of some heterocyclic compound and antioxidant activity. PhD thesis, 2022, University of Thi-Qar.
23. Rasheed M.K., Al-Rifaie D.A. Synthesis some of thiazolidinoneand tetrazole compounds derived from acriflavine and evaluation of their antimicrobial, antifungal and antioxidant activity. *Syst. Rev. Pharm.*, **2020**, 11 (12), 1889-1895. Doi: 10.31838/srp.2020.12.287.
24. Yassin F.A., Seleim A.F. Synthesis and reactions of oxadiazolo, thiadiazolo and triazolo phthalazin- 1(2H)-one derivatives. *Der Pharma Chem.* 2012, **Vol. 4(3)**, p. 860-866.
25. Al-azzawi A.M., Jassem E.K. Synthesis Of Several New Cyclic Imides Linked To [3-Mercapto-5-(4′-tolyl)-1,2,4-triazole] Moiety with Antibacterial Activity Study. *Kerbala J. Pharm. Sci.* 2015, **Vol. 1(10)**, p. 1-14.
26. Al-Mulla A. A Review: Biological Importance of Heterocyclic Compounds. *Der Pharma Chem.* 2017, **Vol. 9(13)**, p. 141-147.
27. Saleh R.H., Rashid W.M., Mohammed A. Synthesis of some new thiazolidinone compounds derived from Schiff bases compounds and evaluation of their laser and biological efficacy. *Ann. Trop. Med. Public Health,* 2020, **Vol. 23(7)**, p. 1017–1031. DOI: 10.36295/ASRO.2020.23728.
28. Constantinos G.N., Ting Z., Alexander D. Tetrazoles via Multicomponent Reactions. *Chem. Rev.* 2019, Vol. 119(3), p. 1970–2042 DOI: 10.1021/acs.chemrev.8b00564.
29. Nikpassand M. Synthesis of fused Azo-linked 1, 2, 4-Triazole-3-Thione derivatives using Ag_2S/RHA-MCM-41 nanocomposite. *Int. J. Nano Dimens.* 2022, **Vol. 13(1)**, p. 117-125. DOI: 10.22034/ijnd.2022.685587.
30. Gotsulya A., Zaika Y. Synthesis, properties and biological potenial some condensed derivatives 1, 2, 4-trizole. *J. Fac. Pharm. Ankara /Ankara Ecz. Fak. Derg.* 2022, **Vol. 46(2)**, p. 308-321. DOI: 10.33483/jfpau.971602.
31. Tornøe C.W., Christensen C., Meldal M. Peptidotriazoles on solid phase: [1,2,3]-Triazoles by regiospecific copper(I)-catalyzed

1,3-dipolar cycloadditions of terminal alkynes to azides. *J. Org. Chem.,* 2002, **Vol. 67(9)**, p. 3057-3064. DOI: 10.1021/jo011148j.
32. Dalal M.J., Mekky A.H. Synthesis, Characterization and Antioxidant Evaluation of Some Tetrazole Derivatives. *Indones. J. Chem.* 2022, **Vol. 22(6)**, p. 1596-1604. DOI: 10.22146/ijc.74912.
33. Pylypenko O.O., Okovytyy S.I., Sviatenko L.K., Voronkov E.O., Shabelnyk K.P., Kovalenko S.I. Tautomeric behavior of 1,2,4-triazole derivatives: combined spectroscopic and theoretical study. *Struct. Chem.* **2023**, **Vol. 34(1)**, p. 181-192. DOI: 10.1007/s11224-022-02057-0.
34. Kumari M., Tahlan S., Narasimhan B., Ramasamy K., Lim S.M. Synthesis and biological evaluation of hetrocyclic 1, 2, 4-triazole scaffolds as promising pharmacological agents. *BMC Chem.* 2021, **Vol. 15(1)**, p. 1-16. DOI: 10.1186/s13065-020-00717-y.
35. Elewa S.I., Fatthallah N.A., Nessim M.I., El-Farargy A.F. Synthesis and characterization of some tetrazoles and their prospective for aerobic micro-fouling mitigation. *Arab. J. Chem.* 2020, **Vol. 13(12)**, p. 8750-8757. DOI: 10.1016/j.arabjc. 10.005.
36. Malik M., Wani A.Y., Shiekh R.A. Tetrazoles as carboxylic acids isosters: Chemistry and biology. *J Incl Phenom Macrocycl Chem*. 2014, **Vol. 78(1-4)**, p. 15-37. DOI: 10.1007/s10847-013-0334-x.
37. Kumar R., Kumar S., Majeed J., Rashid M., Sharma S. Synthesis and in vitro antimicrobial activity of some triazole derivatives. *J. Chil. Chem. Soc.* 2010, **Vol. 55(3)**, p. 359-362. DOI: 10.4067/S0717-97072010000300019.
38. Ansary I., Taher A. *One-Pot Synthesis of Coumarin Derivatives*. Phytochem. Hum. Heal. 2020. DOI: 10.5772/intechopen.89013.
39. Poirot A., Vanucci-Bacqué C., Delavaux-Nicot B., Meslien C., Saffon-Merceron N., Serpentini C.-L., Bedos-Belval F., Benoist E., Fery-Forgues S. Using a diphenyl-bi-(1,2,4-triazole) tricarbonylrhenium(I) complex with intramolecular π–π stacking interaction for efficient solid-state luminescence enhancement. *Dalt. Trans.* 2023, **Vol. 52(17)**, p. 5453-5465. DOI: 10.1039/d2dt03573a.
40. Taydakov I.V., Kreshchenova Y.M., Dolotova E.P. A convenient and practical synthesis of β-diketones bearing linear perfluorinated alkyl groups and a 2-thienyl moiety. *Beilstein J. Org. Chem.* 2018, **Vol. 14**, p. 3106–3111. DOI: 10.3762/bjoc.14.290.
41. Smith K.T., Deblasio J.W., Hamann C.S. *Utilizing NMR To. Study Structure and Equilibrium in the Organic Chemistry Laboratory*. Book chapter 9. ACS Symposium Series. 2016. 2. DOI: 10.1021/bk-2016-1221.ch009.
42. Abd-Alrazzak N., Aowda S.A., Atiyah A.J. Synthesis and Characterization of New 1,2,4-Triazole Derivatives Form 2-Naphthol. *JUBPAS,* 2018, **Vol. 26(6)**, p. 234-252.
43. Ahmed A., Ismaeel Y., Asaad N. Some 3,4,5-Trisubstituted-1,2,4-triazole Synthesis, Antimicrobial Activity, and Molecular Docking Studies. *Egypt. J. Chem.* 2022, **Vol. 65(3)**, p. 395-401. DOI: 10.21608/ejchem.2021.93025.4397.
44. Elgrishi N., Mccarthy B.D., Rountree E.S., Eisenhart T.T. A Practical Beginner's Guide to Cyclic Voltammetry. *J. chem. Educ.* 2018, **Vol. 95(2)**, p. 197-206. DOI: 10.1021/acs.jchemed.7b00361.
45. Liu C., Zhao P., Huang W. New oxadiazole derivatives as promising electron transport materials: Synthesis and characterization of thermal, optical and electrochemical properties. *Cent. Eur. J. Chem.* 2007, **Vol. 5(1)**, p. 303-315. DOI: 10.2478/s11532-006-0052-y.
46. Mohammadi K.H., Babaei A., Sohrabi M. New 1, 2, 4-triazole-based azo – azomethine dyes. Part II: Synthesis, characterization, electrochemical properties and computational studies. *Spectrochim. Acta A Mol. and Biomol. Spectrosc.* 2012, **Vol. 97**, p. 876-884. DOI: 10.1016/j.saa. 07.041.
47. Andrey G.L., Anton V.Y., Konstantin A.L., Frank W.H., Valerii Z.S., Marat M.K. Reversible shifting of a chemical equilibrium by light: the case of keto-enol tautomerism of

a β-ketoester. *Org. Lett.* 2020, **Vol. 22(2)**, p. 604-609. DOI:10.1021/acs.orglett.9b04376.

48. Gatea A.H., Ali S.A., Abdul-Hassan W.S. Comparison study of cloud point and solvent extraction of copper by 3-chloro-2,4-pentanedione as complexing reagent. *Journal of Medicinal and Chemistry Sciences,* 2022, **Vol. 5(5)**, p. 743-752. ID: JMCS-2201-1395.
49. Mehwash Z., Shahid H., Iqbal A., Nida T., Sammer Y. Synthesis, characterization, electrochemical and DNA binding studies of regio-isomeric sulfonyl esters of substituted isoxazoles. *J. of Mol. Struct.* 2020, **Vol. 1202**, 127230. DOI. 1016/j.molstruc.2019.127230.
50. Anastasia S.K., Gabriela W.-S., Aleksandra K., Malgorzata Z., Beata L., Remigiusz G., Ireneusz G., Alexander S.F., Wojciech D., Adam P. Effect of the electron-accepting centre and solubilising substituents on the redox, spectroscopic and electroluminescent properties of four oxadiazoles and a triazole disubstituted with bithiophene. *J Mater Sci*. 2016, **Vol. 51**, p. 2274-2282. DOI: 10.1007/s10853-015-9529-4
51. Daria A.B., Andrey G., Nadezhda P.P., Kristina D.P., Maxim V.A., Oleg P.D., Mikhail A.K., Andrey I.P., Nadezhda T.B., Ivan V.S. Synthesis, electrochemical properties, and antioxidant activity of sterically hindered catechols with 1,3,4-oxadiazole,1,2,4-triazole, thiazole or pyridine fragments. *Beilstein J. Org. Chem.* 2024, **Vol. 20**, p. 2378-2391. DOI: 10.3762/bjoc.20.202.
52. Manna A.H., Goma E.A., Zaky R.R., Eslam A.G., Mahmoud N.A., El-H. Medium controlled redox activity and coordination behavior of a triazole indolinone ligand with vanadyl lons. *Sci Rep.* 2026, **Vol. 16**, 11370. DOI: 10.1038/s41598-026-44306-w
53. Abdul-Hassan W.S., Saint-Aman É., Royal G., Kahlfuss C. Redox- and photo-responsive molecules and molecular materials. *L'ACTUALITÉ CHIMIQUE,* 2018, **Vol. 430-431**, p. 79-84.
54. Azouz J.A., Abdul-Hassan W.S. Synthesis, characterization and redox-responsive novel molecular switching behavior of copper (II)-viologen adduct complexes. *Applied Chemical Engineering*, 2025, **Vol. 8(3)**, 1. DOI: 10.59429/ace.v8i3.5751